Aerosol Science and Technology
Publication details, including instructions for authors and subscription information:
http://www.informaworld.com/smpp/title~content=t713656376

Macrodynamics of Microparticles

Raymond M. Brach [a];Patrick F. Dunn [a]
[a] Particle Dynamics Laboratory, Department of Aerospace and Mechanical Engineering, University of Notre Dame, Notre Dame, IN

First published on: 01 January 1995

To cite this Article Brach, Raymond M. andDunn, Patrick F.(1995) 'Macrodynamics of Microparticles', Aerosol Science and Technology, 23: 1, 51 — 71, First published on: 01 January 1995 (iFirst)
To link to this Article: DOI: 10.1080/02786829508965294
URL: http://dx.doi.org/10.1080/02786829508965294

Macrodynamics of Microparticles

Raymond M. Brach and Patrick F. Dunn
Particle Dynamics Laboratory, Department of Aerospace and Mechanical Engineering, University of Notre Dame, Notre Dame, IN 46566, USA

A primary goal of this paper is to describe the development of two, independent engineering models for the oblique mechanical impact dynamics of solid aerosol particles, treated as microspheres, in the presence of adhesion forces. One model is algebraic and is based on rigid body impact theory* using coefficients such as the coefficient of restitution and the impulse ratio. This model is augmented by an energy conservation expression. Being algebraic and based directly on Newton's laws, the model offers a rigor and simplicity that makes it ideal for analyzing, displaying and interpreting experimental data. Dealing with impulses, this model does not require a detailed knowledge of the forces to analyze energy loss. The second model takes the form of a simulation using the differential equations of planar motion of a sphere in contact with a flat barrier. It uses Hertzian theory for the normal restoring force, an idealized tensile line force around the periphery of the contact region to represent adhesion and Coulomb friction for the force tangent to the surface. Damping with a form of velocity-dependent hysteresis is used both for the material dissipation as well as the energy loss associated with adhesion. Original experimental data from normal and oblique impacts of polydisperse aerosol particles are used to illustrate and compare both impact models. The rigid body model's segregation of dynamic material dissipation (or restitution) and adhesion dissipation allows the latter to be observed as a function of initial normal velocity. Results of this model follow the normally incident data trends quite well. The model also facilitates the interpretation of tangential motion, particularly the conditions of sliding and rolling at separation. Experimental data analyzed with this model indicate that initial angular velocities of microspheres of the order of magnitude of 10^5 rad/s are common and significantly affect the rebound velocities for ordinary levels of friction. Physical constants, calculations and experimental data for silver coated glass spheres colliding with a stainless steel surface are used to estimate the parameter values of the simulation. With these parameters held fixed, the results of the simulation compare quite well to a broad range of experimental data including the transition region from rebound to attachment. The two models predict the impact dynamics almost identically but provide different estimates of the work of adhesion. Improvements of the models in this area are needed and are ongoing.

INTRODUCTION

This paper is a companion to that of Dunn et al. (1995). That paper presents and discusses the results of experiments from both normal and oblique microsphere impacts. This paper develops and discusses two models that describe and predict the impact dynamics of solid aerosol particles. The first model is a variation with some improvements of an algebraic rigid body model already developed by Brach and Dunn (1992). The second, referred to as a simulation, consists of the numerical integration of the equations of motion of the planar mechanics of a deformable sphere colliding with a flat barrier in the presence of friction and adhesion. Each of the models is separately developed in an appendix to this paper. This paper does not contain an extensive

* In dynamics, a distinction is usually made between a point mass and a rigid body; for a rigid body, rotations and the extent of the mass are taken into account. The phrase *rigid body impact theory* in this paper implies the latter and does not imply an absence of deformation.

Aerosol Science and Technology 23:51–71 (1995)

Published by Elsevier Science Inc.

0278-6826/95/$9.50
SSDI 0278-6826(95)00015-8

review of previous work or the status of aerosol impact research; other papers in this volume alreay provide an excellent coverage of this. Instead, several references are cited to help explain some of the motivation for the approaches taken. Over the years, Johnson and his colleagues (Johnson et al. 1971; Johnson and Pollock 1993) have provided fundamental static elastic analyses of a sphere-barrier interaction based on the classical Hertzian formulation of body deformation and extensions to this theory. Their approach has been to model the body deformation as a static or quasi-dynamic process in combination with energy of adhesion associated uniformly with the contact or interface surface. Among the many things learned from Johnson's work, two particular items are noted: a) a ring of extremely high tensile stresses exists on the periphery of the contact area and b) a significant difference exists in the energy lost during the establishment or growth of contact (approach) and during the contraction of the contact area (rebound). Other more recent findings related to energy loss due to adhesion are from the experiments of Horn et al. (1987). A cycle of bringing two surfaces into contact followed by separation shows that significant energy is lost. Their measurements clearly show evidence of adhesion energy loss in the form of hysteresis in the cycle. Originally, it was thought that the dissipation measured may have been due to plastic deformation but private communication with one of the authors and a later publication by Chen et al. (1991) point out that the energy loss is due directly to mechanical hysteresis, chemical hysteresis or a combination of the two associated directly with the adhesion process during separation. This corroborates the observations of Johnson mentioned above.

Another topic of interest is that of plastic deformation. Many existing models of solid aerosol particle impact presume that a significant energy loss comes from plastic deformation in the particle and/or barrier. This mode of deformation usually associated with ductile metals is not pursued here for several reasons. One is that there seems to be little experimental evidence for the existence of significant plastic deformation. Another is that plastic deformation is only one type of material model; the different materials encountered as aerosols (biological materials such as pollens, ash, silicates, polymers, fibers, powders, etc.) presents a wide variety of material behaviors. Also, microparticle impacts occur at tremendously high strain rates which, for ductile materials, evidence (see Biggs 1965; Meyers et al. 1992) indicates that the yield strengths approach the ultimate strengths, the ultimate strengths increase and plastic deformation is minimal. Existing knowledge seems to indicate that dislocations occur with finite velocities and plastic deformation is not an instantaneous process. A 4-μm-diameter metal sphere hitting a hard surface, can have a deformation of the order of 2×10^{-8} m and a (Hertzian) contact duration of the order of 2×10^{-8} s. This corresponds to an average strain rate of the order of 1×10^{6} s^{-1}, orders of magnitude above values typically considered to be "high" for engineering purposes and well above most measured values of dynamic yield strength. A more conventional type of material damping is used in the approach of this paper.

The utility of the rigid body impact model is explored using data from an individual oblique impact from the work of Caylor (1993). These data are used to illustrate the way in which a sphere's velocities are affected in the presence of a tangential retarding force such as Coulomb's friction and how the tangential velocity component and the angular velocity change for various angles of incidence. The rigid body impact model also is used extensively in the companion paper (Dunn et al. 1995) to display and explain the results of numerous oblique and normal

impacts. Note that this model is referred to as a *rigid body* model not to imply that deformations and their effects do not exist, but rather to distinguish it from a *point mass* model where rotational motion is neglected. The rigid body model is derived in Appendix A.

The simulation is explained and illustrated with the use of the data from a large number of normal impacts of polydisperse microsphere experiments as well as the same individual oblique collisions used for the rigid body model. In contrast to the rigid body model, which considers only initial and final values of velocity components, the simulation determines the motion of the microsphere as a function of time during the contact duration. A comparison of the results of the two models allows an evaluation of some of the assumptions made in the derivation of the simpler rigid body model. Some of the important physical parameters of the simulation are estimated using some of the normal impact data of Caylor (1993). Then the simulation is used to calculate solid aerosol particle impact conditions for wide ranges of values of variables and compared to broad ranges of experimental results to assess its efficacy.

A simulation is more of an engineering model and represents a unique approach to the study of microparticle impact. Although some of the processes being modeled are not well understood (such as dynamic energy dissipation associated with adhesion) it is hoped that the model can simultaneously serve as a useful tool for studying solid aerosol impact problems and as a means to investigate new information found from fundamental studies. The derivation of the model's equations and the assumptions made are presented in Appendix B.

RIGID BODY IMPACT MODEL

Brach and Dunn (1992) have presented a rigid body impact model in the past. The current one (see Appendix A) differs from that one in two respects: (1) the previous model did not contain an explicit parameter (coefficient) representing the effect of adhesion; the current approach does, and (2) the previous model used a kinematic (restitution) coefficient for rolling resistance; the current paper uses a kinetic coefficient which is more appropriate since losses due to rolling are not a form of restitution (see Brach 1991 for more discussion on the form of different coefficients). In Brach and Dunn (1992) the rigid body impact model was applied exclusively to normal impact data. In this paper, its use is extended to oblique impacts. This is done using experimetnal data from collisions of silver coated, glass spheres colliding with a flat stainless steel barrier with an uncoated surface. Figure 1 illustrates the configuration and coordinate system of such an impact. Table 1 contains information for an experimentally based representative collision used throughout this paper.

A feature of the notation followed is that when the same symbol is used in both upper and lower case, the lower case variable represents an initial value and the upper case symbol represents the final value. For example, v_n is the normal component of the initial velocity and V_n is the normal component of the final velocity.

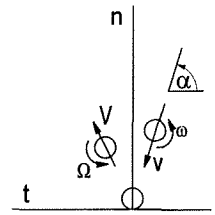

FIGURE 1. Coordinates and notation for microsphere impact dynamics; initial velocities are lower case and find velocities are upper case.

TABLE 1. Representative Normal Collision, Silver-Coated Glass Sphere–Stainless-Steel Surface

Silver-Coated Glass Sphere		Rigid Body Impact Mechanics	
ρ, density	2600 kg/m^3	v_n, initial normal velocity	-2.80 m/s[a]
E, Young's Modulus	72 GPa	v_t, initial tangential velocity	0.00 m/s[a]
ν, Poisson's ratio	0.21	ω, initial angular velocity	1.46×10^5 rad/s[b]
d, diameter	10.12 μm[c]	V_n, final normal velocity	2.09[a]
m, mass	1.41×10^{-12} kg	V_t, final tangential velocity	0.21[a]
k, radius of gyration	3.20 μm	Ω, final angular velocity	4.16×10^4 rad/s[b]
		μ, impulse ratio	0.043[a]
		R, kinetic coefficient	0.978[a]
		e, kinematic coefficient	0.746[a]
Stainless Steel Surface		ρ, adhesion coefficient	0.237[b]
ρ, density	7800 kg/m^3	W_A, work of adhesion fracture	-2.27×10^{-12} J[b]
E, Young's modulus	207 GPa	T_i, initial kinetic energy	5.68×10^{-12} J[a]
ν, Poisson's ratio	0.27	T_L, energy loss	45.1%[a]
z_0, intermolecular distance	4 Å	Maximum Hertzian displacement	1.97×10^{-8} m
		Maximum Hertzian contact radius	3.16×10^{-7} m
		Maximum Hertzian contact force	4.31×10^{-4} N
		Hertzian contact duration	2.07×10^{-8} s
		F_A, average adhesion force	5.43×10^{-5} N[b]

[a]Experiments of Caylor (1993).
[b]Rigid body impact model.
[c]Simulation.

Internal Dissipation in the Sphere and Barrier Materials

The equations of the rigid body impact model from Appendix A provide the final velocities and energy loss in terms of the initial velocities using three coefficients R, ρ, and μ. The coefficient R is based on the compressive restoring force and corresponding dissipation in the absence of adhesion. The deformation grows during the approach phase of the impact and diminishes during the rebound phase. R is defined specifically as the ratio of the rebound impulse of the force of deformation to its approach impulse, the kinetic (or Poisson) coefficient of restitution in the absence of adhesion.

Energy Losses Due to Adhesion

Much of the technical literature on the subject of solid aerosol particle impact seems to concentrate on the mathematical forms of the adhesion force (often limited to the van der Waals force) and the loss of energy due to plastic deformation in the microsphere and/or barrier. According to Johnson and Horn, energy is lost directly when barrier and particle surfaces separate in the presence of adhesion. Little seems to be known about this adhesion "peeling" process. Although *atomic force microscopy* is beginning to provide some valuable information, it still is limited to static rather than dynamic forces. The adhesion process is a contact *surface* phenomenon while the particle/barrier deformation is an internal *body or material* process whose force is transmitted over the same contact surface. It appears reasonable that the energy losses due to adhesion during an impact should be modeled as a process distinct from the body material losses. In the rigid body impact model, this is done using the coefficient R defined above and a separate kinetic coefficient, ρ, which is defined as the ratio of the rebound adhesion impulse to the rebound elastic restoring impulse (itself

determined by R). When the coefficient ρ is zero, there is no energy loss due to adhesion. When the adhesion is strong enough to keep the particle from leaving from the surface, then by definition the adhesion impulse just cancels the restoring impulse and $\rho = 1$. All other cases lie in between; thus $0 \leq \rho \leq 1$. This perspective follows from an assumption that little or no energy is lost through the process of adhesion during the approach phase when adhesion is being established and that energy loss attributed directly to adhesion occurs predominantly during separation, or rebound in the case of impact. On the other hand, if rolling of the sphere takes place during approach (and rebound as well), then the trailing edge of the sphere's surface is peeling from the barrier surface even while adhesion is being established and some energy can be lost. This process has not been discussed before, mainly because studies of adhesion have been limited, by and large, to normal impacts. Chen et al. (1991) relate this effect to rolling friction. Effects of peeling due to rolling are modeled using the ratio of the impulse of the moment (couple) to the normal force impulse over the entire contact duration. Because peeling is at the trailing edge of a changing contact area and the before-and-after nature of the rigid body impact theory cannot take into account the changing contact area a "characteristic moment arm," a_c, is defined and used.

Energy Losses Due to Tangential Retardation

At this point attention is focused on the tangential mechanical process on the sphere–barrier interface. Many possibilities exist including tangential (shearing) elasticity but only retarding forces are considered, that is, forces which cannot do positive work. For example, if the barrier is relatively hard and the contact surface remains flat, then Coulomb friction with coefficient f, could apply. If the sphere is relatively hard and the barrier material is soft, then significant indentation can occur. In this case Coulomb friction may still apply, but now the friction acts over a curved contact surface, a rather complicated process. In general, when both the sphere and barrier are elastic, Coulomb's law is not strictly applicable because incremental slippage can occur (see Jaeger 1994). In some cases, say in the presence of some contaminant or lubricant, viscous friction could even apply. In any case, an advantage of the rigid body impact approach is that a corresponding kinetic coefficient, μ, can be used, independent of the particular tangential process. This coefficient is defined in Appendix A as the ratio of the tangential and normal impulses (not forces, so μ is not necessarily equal to f). The impulse ratio $\mu = P_t/P_n = (V_t - v_t)/(V_n - v_n)$, is easily calculated from experimental data. As discussed by Stronge (1990) the impact of a sphere is a central impact so only two possibilities exist for the motion at separation of the surfaces; these are sliding and rolling. Consequently the coefficient μ can take on only one of two values. If rolling exists at separation, then μ takes on a special, limiting value μ_0, such that

$$\mu_0 = [2(v_t - r\omega)]/[7(1+e)v_n]. \qquad (1)$$

From Appendix A, $e = R(1-\rho)$ is the overall kinematic coefficient of restitution in the presence of adhesion, that is, $e = -V_n/v_n$. Otherwise, if sliding continues throughout the entire collision, μ is determined by the specific tangential retardation process. Suppose that Coulomb friction with a coefficient f applies and that the rotational coefficient μ_m is zero. When sliding exists throughout the contact duration, then $|\mu| = f < |\mu_0|$. Whether or not sliding stops before separation depends on the level of retardation and the initial conditions, particularly the initial tangential velocity at the contact surface.

Note from Eq 1 that μ_0 depends on the initial velocity components.

To examine the utility of the coefficient μ for interpreting experimental data, consider Fig. 2. First consider the special case when the microsphere has no initial spin, that is, $\omega = 0$. Curve 1 shows μ_0 for $R = 0$ as a function of the angle of incidence. Curve II is the same but for $R = 1$ with the two curves forming upper and lower bounds of R. Any sphere (with $\omega = 0$) that is rolling when it rebounds from the barrier surface must have a value of μ that lies between these two curves for its given angle of incidence. A typical data point is shown as point C. Note that if a sphere strikes the surface at an incidence angle of exactly 90° such as point A. With $v_t = \omega = 0$, μ_0 is zero and it must rebound vertically. Now for a given microsphere and barrier suppose the total initial velocity $(v_n^2 + v_t^2)^{1/2}$ is held fixed, still with $\omega = 0$. If the contact interface is not frictionless, for large angles of incidence the sphere will rebound in a condition of rolling. As the angle of incidence is decreased (v_n decreases and v_t increases) the collision becomes more of a glancing one and below some angle, relative tangential motion will continue through the full contact duration. Note that knowledge of the specific nature of the tangential retardation process is unnecessary to make these observations. If Coulomb friction applies then all data points lying below Curve II, such as Point D, are such that $\mu = f$ (suggesting a means for the experimental measurement of f). Suppose that the initial angular velocity, ω, is not zero. Then a normal impact (angle of incidence of 90°) does not necessarily imply a rebound angle of 90° because initial spin can cause a side velocity, V_t, to develop. Curves III and IV are plots of μ_0 for $\omega \neq 0$ and again provide upper and lower bounds for rebounds under the condition of rolling. In general, depending on the sign of ω, the initial rotational inertia can either increase or decrease the final tangential momentum, resulting in either point E_2 or point E_1. For glancing incidence, sliding can still exist at separation and data points will lie below Curve IV such as point D and with extremely high forespin (positive ω), point F.

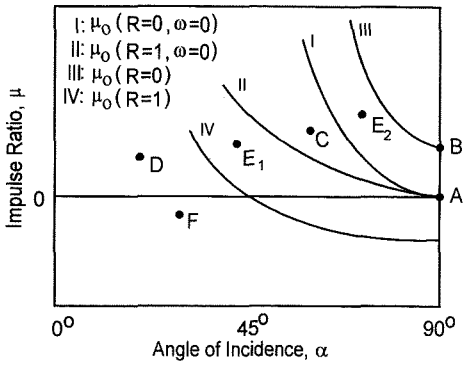

FIGURE 2. The relationship of the impuse ratio μ, its limiting value, μ_0, rebound modes (sliding/rolling) and initial/final spin to angle of incidence.

Example Application of the Rigid Body Model

Consider now a hypothetical collision of a silver coated glass microsphere with a stainless-steel barrier with the conditions listed in Table 1. Most of the conditions for this collision correspond to the actual experimental collision illustrated in Fig. 3, but it is called hypothetical since some of the conditions were unmeasured or otherwise are unknown. For example, the coefficient of friction, f, is unknown and neither the initial nor final angular velocities were measured. Other properties of the collision such as the duration of contact were not measured and are estimated using Hertzian Theory. (The unmeasured mass and diameter was estimated using the simulation, discussed later.) Using the rigid body impact model, some of the unknown conditions can be estimated,

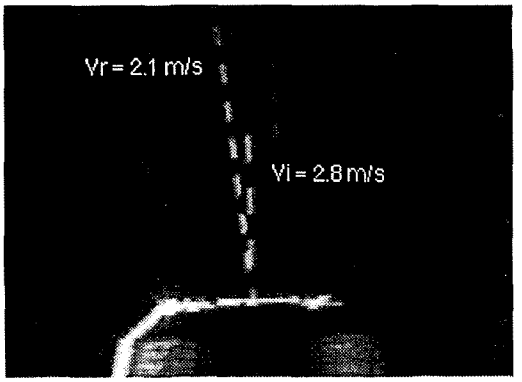

FIGURE 3. Video image of the trajectory of the impact of a silver coated glass particle with a flat, polished stainless-steel barrier at normal incidence (Caylor 1993).

however. Since incidence is normal and rebound is at an angle, this case corresponds to Point B in Fig. 2. The restitution coefficient R is defined here as the restitution of the sphere and barrier materials in the absence of adhesion. Typically, R depends on the initial normal velocity (for example, see Brach 1991). A relatively simple function $R = k/(k + |v_n|)$ adequately represents this relationship. Using the high initial velocity data collected by Caylor, (1993) (where the effects of adhesion are minimal), a value of k of approximately 130 is found. Using the measured initial and final velocity components gives $R = 0.978$. Since $e = 2.09/2.80 = 0.746$ (Fig. 3 and Table 1) then $\rho = 1 - e/R = 0.237$. Consequently, the impulse due to adhesion was about 23.7% of the elastic restoring impulse of the sphere–barrier materials showing that adhesion significantly influenced the rebound velocity. Furthermore, for $\mu = 0.043$ and assuming high enough friction to establish rolling ($f > 0.043$) then $\mu = \mu_0$ and the particle must have had an initial angular velocity of $\omega = 1.46 \times 10^5$ rad/s or greater in order to provide a rebound angle of 5.75°.

Application to Other Data

Figure 4 shows the impulse ratio data of Caylor (1993) for polydisperse stainless-steel microspheres colliding with a flat stainless-steel barrier. At normal incidence ($\alpha = 90°$, $v_t = 0$) values of μ range fairly symmetrically by about ± 0.12 around zero. If a surface is flat and $v_t = 0$,

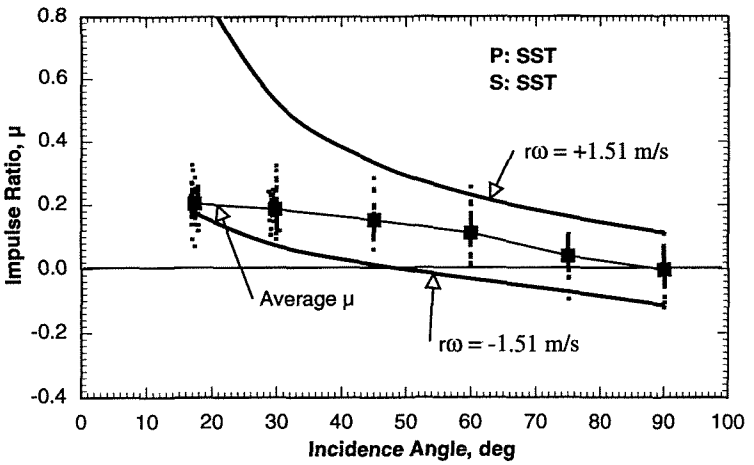

FIGURE 4. Impulse ratios from oblique impacts of stainless steel microspheres (P) against a stainless steel barrier (S) appearing as 6 vertical clusters of points (Caylor 1993).

the only way a tangential impulse can be generated during a normal impact is if the sphere has an initial angular velocity as just discussed. If it is assumed that Coulomb friction is appropriate for these collisions and that the dynamic coefficient of friction is greater than 0.12, then the collisions for all of the 90° data terminated in a rolling mode with $\mu = \mu_0$. For $\mu_0 = 0.12$, Eq. 1 can be used to calculate a corresponding initial angular velocity. Although the impulse ratio is independent of the mass, other quantities do depend on the mass or radius (e.g., angular momentum) so average values must be used in the calculations. The average value of the overall kinematic coefficient of restitution, e, from the 90° data is 0.601. With this information, Eq. 1 gives $r\omega = 1.54$ m/s. This means that the average final tangential velocity, V_t, was about 0.44 m/s (for average normal velocities of -2.3 m/s). For a typical sphere radius of $r = 2.5$ μm, the initial spin must equal 6.2×10^5 rad/s, or 5.9×10^6 rpm. If spin in the presence of friction can induce a tangential velocity, then with the same process, an initial tangential velocity can induce a like spin.

The upper and lower bound curves of Fig. 4 are constant $r\omega$ curves. They diverge because as the incidence angle decreases, the normal velocity component, $v_n = v \sin \alpha$ decreases. Nevertheless, the average value of μ is decreasing and tending toward glancing collisions with sliding throughout the contact duration. Additional discussion of the tangential velocity data from oblique impacts is presented in the companion paper of Dunn et al. (1995).

Attachment or Critical Velocity

An important mode of impact in the presence of adhesion is when the sphere attaches to the barrier. In applications, whether attachment is or is not desirable, the conditions that cause attachment are of interest. When normal impact alone is considered, the condition of attachment typically used is $V_n = 0$ and the initial velocity, v_n, for this condition is often referred to as a critical velocity. If $e = -V_n/v_n$ is the overall kinematic coefficient of restitution and $e = R(1 - \rho)$, then attachment ($e = 0$) corresponds to $R = 0$ or $\rho = 1$. Since attachment occurs at very low velocities, and for most materials, $R \approx 1$ at these velocities, $\rho = 1$ is the governing condition. For oblique (two- or three-dimensional) collisions, the condition of attachment can be more complicated and it may be desirable to define capture or attachment to be when the final kinetic energy of the particle is zero. Based on the equations in Appendix A, and the fact that kinetic energy is related to the sum of squares of the velocity components, this corresponds to the conditions that V_n, V_t, and Ω are each zero. This in turn implies that:

1. $\rho = 1$,
2. $\mu = \mu_0 = (v_t/v_n)/(1 + R)$, and
3. $a_c \mu_m = a_c \mu_{mc} = -\mu_c r(1 + 2r\omega/5v_n)$.

On the other hand, the definition of critical velocity such that $e = 0$ may still be desired for oblique impacts. For most tangential processes, tangential contact motion is dependent on normal motion, but not vice versa. See the System Equations in Appendix A where it is seen that the equations for the unknown normal velocity can be obtained without solving for the tangential and rotational velocity components. Since *any* retarding tangential process (and rolling process) must dissipate energy its presence should never increase the critical velocity. It is conceivable that a sphere could attach yet continue to roll on a flat barrier surface, eventually coming to rest. For a near-frictionless condition, it is even possible for a sphere to not leave the surface but continue to slide. If the presence of a tangential velocity com-

ponent enhances rebound as some experimental evidence suggests, it is likely because of a secondary effect such as sliding combined with surface roughness decreasing the establishment of the adhesion bond. This topic needs additional study.

Discussion

To place the rigid body model into perspective, note that it is a model of the impact dynamics, not an adhesion or friction, or body elasticity model. It includes the effects of these processes through the use of coefficients without explicitly modeling the contact processes. By using these coefficients the model achieves simultaneously a great simplicity and great generality. When set up properly, a distinct coefficient represents each of the significant physical processes. In addition to being a predictive model, it can serve as a means of organizing and examining experimental data. The use of the model with experimental data can help identify the characteristics of a process. Through each coefficient, deformational, adhesion and frictional energy losses can be estimated and compared to various process theories and models. As pointed out in by Brach and Dunn (1992) the rigid body impact model is not isolated from process models.

DYNAMICAL SIMULATION

Appendix B contains a detailed derivation of a set of three second-order, ordinary differential equations for the motion of a deformable microsphere striking a barrier. The dependent variables are the normal deformation, tangential displacement and rotational displacement of the sphere, $n(\tau)$, $t(\tau)$, and $\theta(\tau)$, respectively, where τ represents time. The (elastic) restoring force is assumed to be that from Hertzian theory given by $\sqrt{r}Kn^{3/2}$ and the damping is assumed to have a hysteretic nature given by $\sqrt{r}Kn^{3/2}c_H\dot{n}$, where $\dot{n}$ is the normal velocity of the mass center of the microsphere. The adhesion force is modeled as an uniformly distributed line force acting over the circumference of the contact radius with magnitude, $2\pi af_0$, where a is the radius of the (circular) contact area and f_0 is the strength of the distributed force. A similar form of dissipation as above $2\pi af_0c_A\dot{n}$ is used for adhesion except that the damping coefficient c_A is set to zero during the establishment of adhesion (the approach phase of the impact). The tangential process used in the simulation is that of Coulomb friction with a dynamic coefficient f, where the tangential force opposes the relative velocity with a magnitude of $f\sqrt{r}Kn^{3/2}$ during sliding, or is zero when the sphere is rolling. Note that the Hertzian stiffness is the only parameter which can be calculated from physical properties of the microsphere. The adhesion parameters, c_A and f_0, the material dissipation, c_H and the friction coefficient must be determined experimentally.

Nondimensional damping constants ζ_H and ζ_A are used in the model in place of c_H and c_A, respectively. These (ζ_H and ζ_A) are developed in Appendix B by multiplying each c_i by the ratio of the Hertzian contact duration, T (see Timoshenko and Goodier 1951) to the microsphere radius, giving $\zeta_H = c_HT/r$ and $\zeta_A = c_AT/r$.

Normal collisions of polydisperse silver coated glass microspheres against a stainless-steel barrier are used to illustrate the simulation and compare its results to experimental data. The coefficients K, f_0, c_A, and c_H (or ζ_A and ζ_H) described above must be determined to run a simulation; a procedure is now outlined. A value of the sphere radius of 4.3 μm was selected corresponding to the arithmetic mean value of Caylor (1993). An initial normal velocity of -2.8 m/s was then chosen as being in the range where adhesion effects are significant. The Hertzian stiffness, $K = 7.5 \times 10^{10}$ N/m^2 was calculated from the

physical properties of the sphere and barrier. A range of f_0 was then estimated by using static equilibrium conditions. Figure 5 is a photograph of some silver-coated glass microspheres on a stainless-steel surface following impact. It is estimated visually that the contact radius a of the largest microsphere is, very roughly, about 5%–10% of its radius. For the static equilibrium condition, Eq. B6 gives $f_0 = Kn_{eq}/2\pi = Kr(a_{eq}/r)^2/2\pi$. This leads to a range of values of 128.3 to 513.3 for f_0 with a geometric mean of 256.6. Based on this, a value of $f_0 = 250$ N/m was chosen for the simulation. First, the simulation was run with $f_0 = 0$, choosing ζ_H by trial and error until it matched the value from the experimental measurements. [In effect, this amount to fitting the value of the material restitution, R. See the companion paper by Dunn et al. (1995) for more information.] This gave a value of ζ_H of 10.45. Now, by trial and error, using $f_0 = 250$, the simulation leads to a value of $\zeta_A = 12.5$ that produces an overall restitution coefficient $e = 0.62$, the experimental value corresponding to $v_n = -2.8$. From this point on, the values of the four parameters were held fixed for all of the remaining calculations.

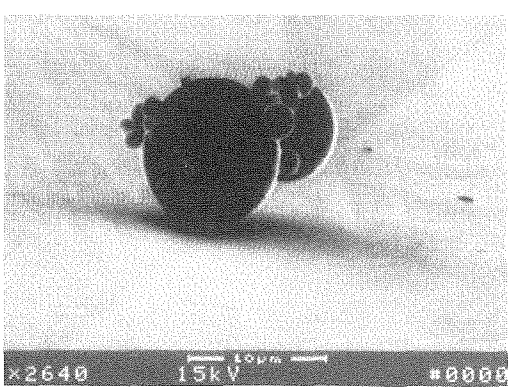

FIGURE 5. Postcollision scanning electron microscope photograph of silver coated, glass microspheres in contact with each other and a stainless steel barrier surface.

Varying the initial normal velocity produced the curves in Fig. 6 for diameters of 5 and 13 μm. The simulation predicts capture for the 5-μm microsphere for an initial velocity of $v_n = 5$ m/s. Capture motion predicted by the simulation consists of a damped oscillation about a static equilibrium deformation of 2.09×10^{-8} m computed from $n_{eq} = 2\pi f_0/K$. The simulation indicates that the capture or critical velocity depends significantly on the size (mass) of the particle.

Now consider the oblique impact of the single microsphere corresponding to the conditions in Table 1. Here, a normally incident microsphere rebounds at an angle of 5.75°, due to the presumed existence of an initial angular velocity. According to Table 1, the experimental impulse ratio is $\mu = 0.043$. Assuming that the governing tangential process is Coulomb friction, this means that for any value of a coefficient of friction $f > 0.043$, the sphere will be rolling (instead of sliding) at separation. A value of $f = 0.1$ is used in the simulation. The results of the simulation (using the same values of K, f_0, ζ_H, and ζ_A as above) give identical final conditions as the rigid body example in the previous section including a rebound angle of 5.75°. In addition, the motion during the contact duration is shown in Figs. 7–9.

Discussion of the Simulation Model

The main features of the simulation model include a compressive elastic Hertzian reaction force and a circumferential tensile adhesion force, both mechanically conservative. In addition, the model includes dissipation terms in the form of the product of the displacement and normal velocity, both providing a hysteretic type of damping. A final feature is the nondimensional form of the damping coefficients.

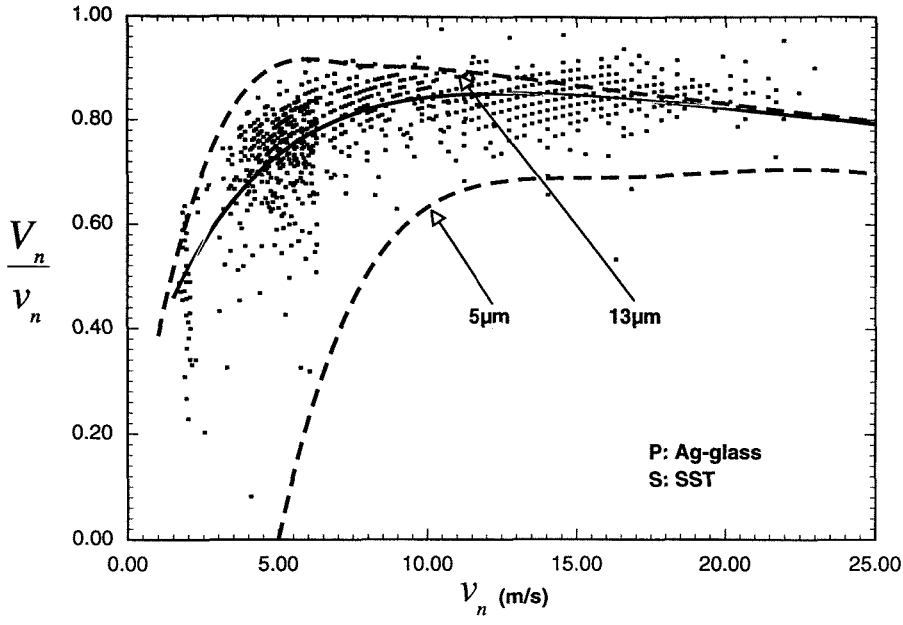

FIGURE 6. Experimental velocity ratios (shown as points) of normally incident polydisperse silver coated glass microspheres (Caylor 1993); dashed curves show results from the dynamical simulation and the solid curve is from the rigid body impact model (Table 1).

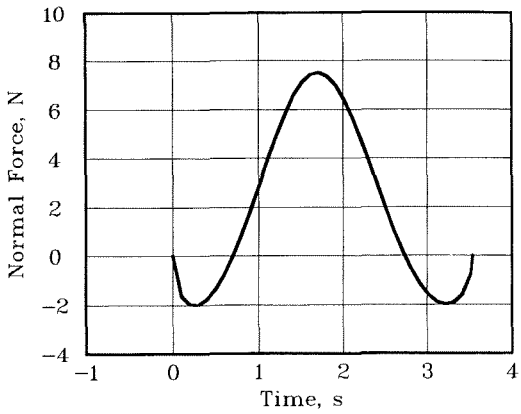

FIGURE 7. Simulated normal force as a function of time for the conditions of Table 1 using $K = 7.5 \times 10^{10}$ N/m^2, $f_0 = 250$ N/m, $\zeta_H = 10.54$, and $\zeta_A = 12.50$; time is normalized to 10^{-8} s and the force is normalized to 1×10^{-4}.

By and large, this combination provides a model that follows the trends of experimental data quite well. From Fig. 6, it appears that there may be a vertical bias or offset of the model restitution from the data since the upper curve should include about 90% of the data based on the mass distribution of the polydisperse particles. The bias or offset could be due to the process used to fit the model parameters, particularly f_0, but it could also be due to inadequacies of the model. Since the simulation requires a numerical solution, it does not provide analytical expressions for such quantities as the critical velocity; their determination requires a trial-and-error process. This is not a severe problem since the solution time on a microcomputer takes less than a minute.

The model cannot provide stress distributions but has the capability of displaying the behavior of the different resultant forces acting over the contact surface and

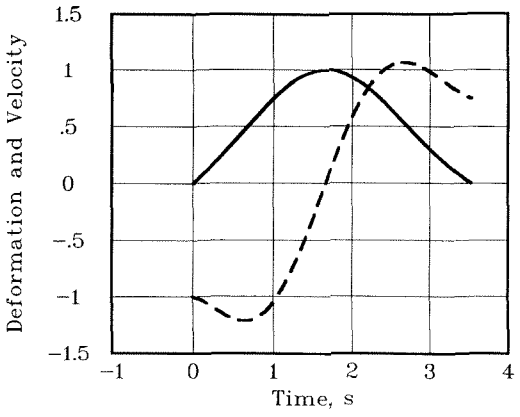

FIGURE 8. Displacement (solid curve) and velocity (dashed curve) of the mass center of a 10.12-μm-diameter microsphere from a simulation corresponding to the conditions of Table 1; the displacement is normalized to its maximum value of -4.243×10^{-8} m, the velocity is normalized to its initial value of 2.8 m/s, and time is normalized to 10^{-8} s.

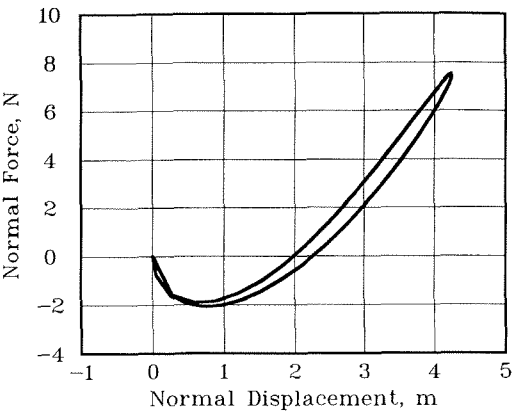

FIGURE 9. Hysteresis loop of the net normal force and the mass center displacement from the simulation for the conditions of Table 1; the normal force is normalized to a value of 1×10^{-4} and the displacement is normalized to a value of 1×10^{-8}.

the consequent deformation and velocities during the contact duration. Figure 7, for example shows that the adhesion force plays a dominant role in the early and late parts of the impact, whereas the compressive body reaction force is dominant during the mid portion. Currently the simulation does not predict any "snap off" as discussed by Johnson and Pollock (1993). This phenomenon can be included in the model once the mechanism and its parameters (such as the force/stress at which the tensile bond "breaks") are known. The deformation and velocity curves of Fig. 8 provide no surprises, other than that adhesion early and late in the contact duration causes a notable increase in the approach velocity and attempt to "return" the microsphere to the surface during rebound. Figure 9 shows that the form chosen for the dissipation terms does indeed provide hysteresis where the energy loss is the area enclosed by the loop in the curve. This curve can be compared to the corresponding (static) experimental curve in Horn et al. (1987); the curves have almost identical characteristics.

One of the results from the simulation not presented is that the rebound angle was 5.76°, the same as the experimental value in Table 1. In some ways this perfect agreement is not surprising since the value used for the initial angular velocity of 8.34×10^6 deg/s was found from the rigid body model using μ_0. On the other hand, that the simulation and rigid body model both gave the same rebound angle (as well as all *identical* final velocities and total energy loss) points out that overall the rigid body model is quite accurate. In addition, the simulation showed that the angular rotation (rotational displacement) during the contact duration was 0.12 degrees. This supports the assumption made in the derivation of the rigid body model of negligible displacements and finite velocity changes.

An area not showing good agreement between the simulation and the rigid body impact model is related to the assumption (for the rigid body model) of the indepen-

dence of the body force and the adhesion force. The two models do not predict the same amount of work in overcoming the adhesion force during rebound. From Table 1, the rigid body model adhesion work is -2.27×10^{-12} J, whereas the simulation gives a value of -4.83×10^{-13} J. This difference is likely because the presence of adhesion during approach causes a greater microsphere deformation and corresponding dissipation. This will be explored in the future, since it may be possible to change the rigid body model to bring in interaction between the coefficients R and ρ. Figure 8 shows that the presence of adhesion increases the approach velocity (and kinetic energy) resulting in greater deformation in the microsphere than occurs in the absence of adhesion. The rigid body model deformation (using Hertzian theory) from Table 1 is 1.97×10^{-8} m whereas the simulation value is 4.24×10^{-8} m. Nevertheless, according to Fig. 6, the rigid body model seems to follow the experimental trends quite well. More detailed comparisons of the two models will be made as they are used to analyze additional data in the future.

CONCLUSIONS AND RECOMMENDATIONS

Both of the models of microsphere dynamics presented in this paper are useful to study the behavior of microspheres. The rigid body model is algebraic and simpler, making it more suitable to use for the display and analysis of experimental data. It provides values of the work of adhesion and can predict the critical velocity (see Brach and Dunn 1992). The simulation on the other hand can do all that the rigid body model does and additionally provide a better understanding of how parameter changes affect the actual motion of the microsphere during contact. By modifying the simulation equations, different theories of how energy is dissipated can be compared. Some of this is planned for future research.

Note that models containing rotational motion are necessary to study whether or not rotational dissipation is significant. This capability is already in the rigid body model and adding it to the simulation is relatively simple. Unfortunately, experimental measurements need to be made and involve measuring the rotational velocities and displacements of microspheres, something that has yet to be done and could be quite challenging.

Extensions of both models to three dimensions is planned to follow up on the current research. In addition, extensions to nonspherical bodies is also planned. Extending the simulation to nonspherical bodies is simpler because the rigid body model becomes complicated because of a great number of stick-slip conditions, including the possibility of tangential contact velocity reversals (see Stronge 1990).

APPENDIX A: EQUATIONS OF A PLANAR IMPACT OF A SPHERE IN THE PRESENCE OF MICROFORCES

Introduction

The methods of rigid body impact are applied in this appendix to the problem of a sphere colliding with a flat immovable barrier. The approach uses the techniques developed by Brach (1991, 1991a) and takes advantage of the simplicity of algebraic solutions for collisions that occur over short periods of time. The assumption of a short contact duration implies large contact forces, negligibly small displacements and finite velocity changes. The primary intent of the following is to provide a model of the *impact dynamics* of a microsphere in the presence of microforces so that experimental results of Caylor (1993) and others can be meaningfully evaluated.

Notation

A as a subscript, adhesion; as a superscript, indicates approach
a_c characteristic moment arm for rolling dissipation
B adhesion energy loss parameter
C point in the contact area through which impulses act
D as a subscript, indicates sphere deformation
e overall restitution normal to the surface
$F(\tau)$ force as a function of time
F_n normal reaction force component due to deformation of the sphere
F_A normal force component due to an adhesion force
F_E normal force due to arbitrary, but known external microforces (other than F_A)
$g(\tau)$ couple (moment) acting over the contact surface due to adhesion
k centroidal radius of gyration of the sphere
M_A impulse couple of $g(\tau)$ due to rolling in the presence of adhesion
$m(\tau)$ impulse of $g(\tau)$ as a function of time
m mass of the sphere
n normal coordinate
P impulse of a force over a specific interval
$p(\tau)$ impulse of a force as a function of time
r radius of the sphere
R kinetic coefficient of restitution resulting from losses due to internal dissipation
R as a superscript, indicates rebound
T_L kinetic energy loss
t tangential coordinate
V velocity at the end of a specific interval
v velocity at the beginning of a specific interval
$\bar{v}$ velocity at time $\tau = \bar{\tau}$
$v(\tau)$ velocity as a function of time
W mechanical work
θ rotational coordinate
μ ratio of impulse components
η velocity ratio, defined in Eq. A28
ρ coefficient relating the adhesion and body impulses during rebound
τ time
$\bar{\tau}$ the time separating approach and rebound
Ω angular velocity at the end of impact
ω angular velocity at the beginning of a specific interval
$\omega(\tau)$ angular velocity as a function of time
$\bar{\omega}$ angular velocity at $\tau = \bar{\tau}$

Analysis

Figure A1 shows a planar, n–t–θ, coordinate system and a sphere contacting a flat surface during an impact. The forces acting at the contact interface in the normal direction include a force due to body deformation, $F_D(\tau)$, an adhesion force, $F_A(\tau)$ and other microforces (such as electrical charge forces), $F_E(\tau)$. These actually are resultant forces of stresses distributed over the contact surface. A tangential force, $F_t(\tau)$, and a couple or moment, $g(\tau)$, is

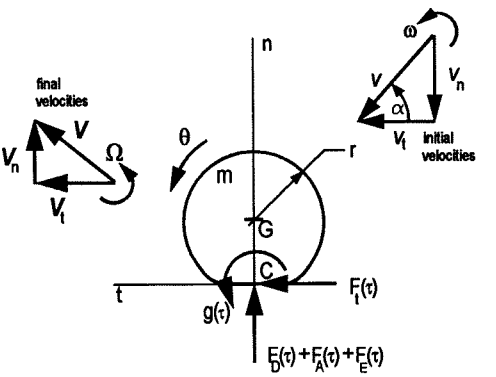

FIGURE A1. Free body diagram of a sphere in contact with the surface of a flat immovable barrier.

included. It is assumed that these arise from distinct physical processes which act over the contact interface. For rigid body impact theory, the forces are not treated explicitly, but rather their impulses. In general, the indefinite impulse of a force is given as

$$p(\tau) = \int_0^{\tau} F(\tau)\, d\tau. \tag{A1}$$

Using this concept, Newton's second law applied to the normal forces and tangential forces over an arbitrary duration of time 0 to τ gives, respectively:

$$m v_n(\tau) - m v_n = p_n(\tau) = p_D(\tau) + p_A(\tau) + p_E(\tau), \tag{A2}$$

$$m v_t(\tau) - m v_t = p_t(\tau). \tag{A3}$$

For rotational motion, the corresponding equation is

$$mk^2\omega(\tau) - mk^2\omega = -r p_t(\tau) + m(\tau). \tag{A4}$$

Equations such as these can be used to model a variety of physical problems conforming to Fig. 1, such as a paddle hitting a ping-pong ball. It is assumed here though that the surface hit by the sphere is stationary and cannot transmit kinetic energy to the sphere. These equations are now evaluated over 2 particular phases of the impact, namely, approach and rebound.

System Equations. Before finding the system equations a simplifying assumption is made, namely that the impulse due to establishment of adhesion is negligible (during the approach phase). In effect, this assumption means that the coupling between the adhesion force and body deformation (and dissipation) is negligible. Let the approach phase of the impact be from $\tau = 0$ to $\tau = \bar{\tau}$ and the rebound phase be from $\bar{\tau}$ to τ_f, where $v_n(\bar{\tau}) = \bar{v}_n = 0$. Then for the approach phase,

$$m(0 - v_n) = P_D^A + P_E^A, \tag{A5}$$

$$m(\bar{v}_t - v_t) = P_t^A, \tag{A6}$$

$$mk^2(\bar{\omega} - \omega) = -rP_t^A + M_A^A, \tag{A7}$$

where P_D^A, P_t^A, and P_E^A are the impulses of the corresponding force components shown in Fig. A1. For the rebound phase,

$$m(V_n - 0) = P_D^R + P_A^R + P_E^R, \tag{A8}$$

$$m(V_t - \bar{v}_t) = P_t^R, \tag{A9}$$

$$mk^2(\Omega - \bar{\omega}) = -rP_t^R + M_A^R. \tag{A10}$$

Following the rigid body approach, it is necessary to define coefficients to provide more system equations so that a sufficient number is available to solve for the unknowns. In general, 1 coefficient (and equation) is necessary for each unknown impulse component. Two types of coefficients can be used. A *kinematic* coefficient is typically defined as a ratio of two velocities and a *kinetic* coefficient as a ratio of two impulses. For additional discussion, see Brach (1991a) and Stronge (1990). A kinetic coefficient of restitution representing internal dissipation (in the absence of microforces) in the sphere, sometimes referred to as Poisson's coefficient is defined as R giving

$$P_D^R = RP_D^A, \quad 0 \le R \le 1. \tag{A11}$$

The ratio of a tangential impulse component to the corresponding normal impulse component over approach and rebound phases give the equations

$$P_t^A = \mu^A\left(P_D^A + P_E^A\right), \tag{A12}$$

$$P_t^R = \mu^R\left(P_D^R + P_A^R + P_E^R\right), \tag{A13}$$

where μ^A and μ^R are impulse ratio coefficients. It should be noted that these equations and coefficients are not dependent on the specific nature of the tangential forces. For example, the tangential

force $F_t(\tau)$ and its impulses P_t^A and P_t^R may be due to dry friction, viscous friction or other process. Knowledge of the relationship of the μs to a process is not necessary to formulate the system equations or obtain their algebraic solution. Ultimate determination of these coefficients requires analytical modeling of the process and/or experimental data, however.

Let ρ be the ratio of the adhesion impulse to the body impulse during rebound, then

$$P_A^R = -\rho P_D^R. \tag{A14}$$

Finally, approach and rebound coefficients that represent dissipation due to adhesion during rolling are defined by the equations

$$M_A^A = \mu_m^A a_c P_D^A, \tag{A15}$$

$$M_A^R = \mu_m^R a_c P_D^R. \tag{A16}$$

At this stage in the derivation, there are 12 unknowns and 12 equations. The unknowns are: V_n, V_t, Ω, $\bar{v}_t$, $\bar{\omega}$, P_D^A, P_D^R, P_t^A, P_t^R, P_A^R, M_A^A, and M_A^R. Equations A5–A16 form a set of 12 linear algebraic equations in these unknowns called the system equations.

Expressions for the normal, tangential and rotational velocity changes over the full duration of the impact, can be derived from Eqs. A2 and A3 or found from combinations of Eqs. A5–A10; these and the tangential impulse equation are

$$m(V_n - v_n) = P_D + P_E + P_A = P_n, \tag{A17}$$

$$m(V_t - v_t) = P_t, \tag{A18}$$

$$mk^2(\Omega - \omega) = -rP_t + M_A, \tag{A19}$$

$$P_t = \mu(P_D + P_A + P_E) = \mu P_n, \tag{A20}$$

where the impulse ratio μ corresponds to the entire duration of contact.

Solution Equations. Before finding the solution of the system equations a simplifying assumption is made that the external forces are absent, $F_E(\tau) = 0$. Since these are considered here to be known quantities, they could be carried along, but are dropped for the remainder of the analysis. Expressions from the solution equations for some of the unknowns of interest are:

$$V_n = -R(1-\rho)v_n, \tag{A21}$$

$$V_t = v_t - \mu[1 + R(1-\rho)]v_n, \tag{A22}$$

$$\Omega = \omega + 5(\mu r - \mu_m a_c)[1 + R(1-\rho)]v_n / 2r^2, \tag{A23}$$

$$P_D = -m(1+R)v_n, \tag{A24}$$

$$P_A^R = \rho R m v_n. \tag{A25}$$

Note from Eq. A21 that the kinematic coefficient of restitution $e = -V_n/v_n = R(1-\rho)$. An important auxiliary expression is for the tangential contact velocity, V_{Ct}, at point C. If this becomes zero at any time during the impact, the mode of motion of the sphere changes from sliding to rolling. This velocity is $V_{Ct} = V_t - r\Omega$ and can be expressed as

$$V_{Ct} = v_t - r\omega - (7\mu/2 - 5\mu_m a_c/2r) \times [1 + R(1-\rho)]v_n. \tag{A26}$$

The impulse ratio, μ_0, just large enough to cause rolling, or $V_{Ct} = 0$ is

$$\mu_0 = 5\mu_m a_c/7r + 2\eta/7[1 - R(1-\rho)] \tag{A27}$$

where

$$\eta = (v_t - r\omega)/v_n. \tag{A28}$$

If the tangential process is one of retardation, dependent upon relative tangential velocities across the interface, Eqs. A26–A28 can be interpreted in the following way. If sliding exists initially (which is typically the case) the force $F_t(\tau)$ may or may not cause sliding to end (and rolling to begin) during the contact duration. The greater the (tangential) retardation or friction, the greater the value of P_t and the impulse ratio μ for given initial conditions. Once rolling begins, however,

the retardation force essentially diminishes, $p_t(\tau)$ no longer increases and the value of μ is at its maximum value, μ_0. Thus, μ_0 serves as a bound on μ. In the absence of rolling dissipation ($\mu_m = 0$), $|\mu| \leq |\mu_0|$. (Since μ can be either positive or negative, absolute values must be used.) When rolling dissipation is present, other bounds based on conservation of energy must be established.

Work and Kinetic Energy. An important expression found from the solution equations is for the kinetic energy lost during the collision. It is found by subtracting the final kinetic energy from the initial using the solution equations to express final velocities in terms of the initial velocities and the coefficients. Using e in place of $R(1-\rho)$, this is

$$2T_L/mv_n^2 = (1-e^2) - \mu^2(1+e)^2 + 2\mu(1+e)\eta - 5(\mu r - \mu_m a_c)^2 \times (1+e)^2/2 + 2\mu_m a_c \omega \times (1+e)/v_n. \quad \text{(A29)}$$

In general the work of an impulse is given by

$$W = \int F\,dx = \int F(\tau)\dot{x}\,d\tau = \int v(\tau)\,dp. \quad \text{(A31)}$$

For example, consider the special case of normal impact. Substituting for $v(\tau)$ from Eq. A-2 with $p_A(\tau) = p_E(\tau) = 0$ and integrating over the approach phase shows that the work done by the normal impulse during approach is $W^A = -\frac{1}{2}mv_n^2$. Similarly, the work of the impulse P_D^R (the rebound impulse due to the sphere's body forces) is found to be $\frac{1}{2}R^2(1-\rho)mv_n^2$. The work, W_A, of P_A^R, the rebound adhesion impulse is $-\frac{1}{2}R^2\rho(1-\rho)mv_n^2$. Note that when the adhesion impulse is strong enough for the adhesion to capture the particle, $\rho = 1$, indicating that the adhesion impulse is equal (and opposite) to the sphere's restoring impulse. By equating the kinetic energy gain to the total work of the normal impulse for the entire contact duration, an energy-based relationship between restitution coefficients for normal impacts is obtained, i.e.,

$$e^2 = R^2(1-\rho)^2 \quad \text{(A32)}$$

Figure A2 shows the generic behavior of these impact restitution coefficients as the initial normal velocity changes. Rigid body impact theory is incapable of providing separate expressions for the the work of body dissipation and the work of adhesion. Consistent with the assumptions made above an energy conservation equation can be written as

$$(1-e^2)\tfrac{1}{2}mv_n^2 = (1-R^2)\tfrac{1}{2}mv_n^2 + W_A. \quad \text{(A33)}$$

The term on the left is the total kinetic energy loss. The first term on the right is the energy lost due to dissipation in the sphere and the last term is the work done in fracturing the adhesion bond during rebound. Dividing by the initial kinetic energy and simplifying gives

$$e^2 = R^2 - B, \quad \text{(A34)}$$

where B is $2W_A/mv_n^2$, the ratio of the work of overcoming adhesion to the ki-

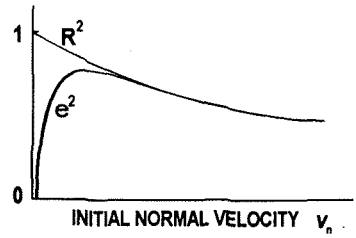

FIGURE A2. Generic behavior of energy restitution for common materials.

netic energy associated with the initial normal velocity.

APPENDIX B: SIMULATION OF A PLANAR IMPACT OF A SPHERE IN THE PRESENCE OF ADHESION

Introduction

This appendix contains a description of a model and its corresponding equations which permits a dynamic simulation of a planar collision of a sphere with a flat rigid barrier. The sphere is assumed to be deformable with a size small enough that adhesion forces are significant. The mechanics of the deformable sphere are based on Hertzian theory. The adhesion force is considered to be a surface force whereas the Hertzian restoring force is due to the deformation of the body of the sphere, transmitted over the contact surface. The combination of the two force systems is assumed to form an idealized ring of tensile adhesion around the periphery of a circular area of compression. Current literature provides mathematical models of the Hertzian restoring force (Timoshenko and Goodier 1951) and the van der Waals adhesion force (Israelachvili 1985) that are conservative, that is, no energy is lost. Experimental data show otherwise, of course, so dissipation is included in the model for a realistic simulation. Dissipation for the Hertzian and adhesion forces is given the form of hysteresis with the mathematical form suggested by Hunt and Crossley (1975).

The simulation is one based on differential equations and has a level of complexity such that numerical integration is necessary for solutions. Even so, it is relatively crude from a perspective of continuum theory. For example, no tangential deformation is considered and coupling between the normal and tangential surface forces and deformation is not considered directly. Elasticity models for impact do exist, such as the one of Jaeger (1992, 1994), but are beyond the scope of this paper. In essence, the model in this appendix should be viewed as a simple, one degree-of-freedom system where impact is considered to be a half cycle of vibration. It contains representations of the major process parameters based on simplifying assumptions discussed in the derivation. The intention is to estimate the normal, tangential and rotational displacement of the sphere as a function of time during the period of contact and to estimate the conditions for attachment. The results of the model are complementary to the *rigid body impact model* also presented in this paper and both are compared with the experimental results reported in Part II of this paper.

Notation

$a(\tau)$	Hertzian contact radius
$a_c(\tau)$	characteristic moment arm
c	dissipation rate
E	modulus of elasticity
$F(\tau)$	force as a function of time
f	coefficient of dynamic friction
f_0	magnitude of adhesion line force
$g(\tau)$	couple (moment) acting over the contact surface due to adhesion
K	Hertzian elastic constant
k	centroidal radius of gyration of the sphere
k_i	elastic constant (sphere and barrier)
m	mass of the sphere
n	normal coordinate
r	radius of the sphere
T	Hertzian contact duration
T_L	kinetic energy loss
t	tangential coordinate
θ	rotational coordinate
τ	time
λ	peeling moment parameter
ζ	nondimensional dissipation parameter
ν_i	Poisson's ratio (sphere and barrier)

Equations of Motion

Figure B1 shows a cross section of a deformed sphere colliding with a flat rigid surface over a circular contact area of radius a. Compressive, tensile and shearing stresses act over the contact area. The compressive stresses are a result of the deformation of the sphere, the tensile stresses are due to adhesion attraction and the tangential are due to resistance to slip over the surface. The resultant of the compressive stresses is modeled as a Hertzian elastic force with dissipation. The net tensile resultant of the adhesion force is modeled as a ring force at the periphery of the (changing) contact area, also with a dissipation term. The resultant of the tangential (shearing) stresses is modeled simply as dry, Coulomb, friction. Dry friction is not strictly appropriate since the contact here is not between 2 rigid bodies, but any other more exact model would add considerable complexity and is withheld for later study.

Based on Hertzian theory and the damping force model of Hunt and Crossley, an equation of motion for the normal displacement of the mass center of the sphere is

$$m\ddot{n} = -\sqrt{r}\,Kn^{3/2} - \sqrt{r}\,Kn^{3/2}c_H\dot{n} + 2\pi a f_0 + 2\pi a f_0 c_A \dot{n}. \tag{B1}$$

Of the terms on the right hand side, the first is the classical Hertzian restoring force and the second is a dissipation term. Also

$$K = 4/3\pi(k_1 + k_2)^2 \tag{B2}$$

and

$$k_i = (1 - \nu_i^2)/\pi E_i. \tag{B3}$$

The third term of Eq. B-1 represents an idealized adhesion attraction as a conservative circumferential (line) force. The last term adds dissipation due to adhesion in the form of hysteresis. The contact radius, a, is related by Hertzian theory such that $a^2 = rn$.

The damping terms are modified by placing the dissipation parameters into nondimensional forms. The strength of the Hertzian dissipation rests in the magnitude of the constant c_H. A nondimensional parameter ζ_H is defined such that

$$\zeta_H = rc_H/T = c_H\left(r^3 K v_n^{1/2}/m\right)^{5/2} \tag{B4}$$

where T is the period of contact predicted by Hertzian theory. Similarly, a nondimensional dissipation parameter is defined for the adhesion term as

$$\zeta_A = rc_A/T = c_A\left(r^3 K v_n^{1/2}/m\right)^{5/2}. \tag{B5}$$

In order for ζ_A to be considered a constant it is necessary to assume that $n(\tau) \approx n_0$ in the nondimensionalizing process. Using these dissipation coefficients, the final form of Eq. B1 then becomes

$$m\ddot{n} = -\sqrt{r}\,Kn^{3/2}\left[1 + \zeta_H\left(m/r^3 K v_n^{1/2}\right)^{2/5}\dot{n}\right] + 2\pi\sqrt{rn}\,f_0\left[1 + \zeta_A\left(m/r^3 K v_n^{1/2}\right)^{2/5}\dot{n}\right] = F_n(\tau). \tag{B6}$$

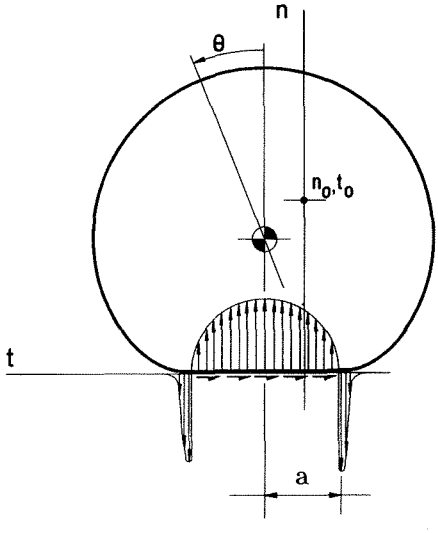

FIGURE B1. Contact surface stresses acting on a deformed sphere.

The adhesion force is not derived from basic principals and represents an idealization of the force as described by others (for example, see Johnson and Pollock 1993; Fichman and Pnueli 1985) and that has been proposed by Brach and Dunn (1992). The quantity f_0 is not necessarily constant but is assumed to be constant here. Finally, there seems to be very little information in the current literature concerning the mathematical nature of dissipation due to adhesion. It is assumed here that no significant adhesion dissipation occurs during establishment of adhesion, that is, during approach, so that $\zeta_A = 0$, $\dot{n} < 0$.

The tangential motion at the contact surface is either sliding or no sliding (rolling). Based on the assumption of dry friction, the equation of tangential motion is

$$m\ddot{t} = F_t(\tau), \tag{B7}$$

where

$$F_t = -f\sqrt{r}\,Kn^{3/2}\,\mathrm{sgn}(\dot{t} - r\dot{\theta}), \qquad \dot{t} - r\dot{\theta} \neq 0 \tag{B8a}$$

and

$$F_t = 0, \qquad \dot{t} - r\dot{\theta} = 0. \tag{B8b}$$

The equation of rotational motion is

$$mk^2\ddot{\theta} = -rF_t(\tau) + g(\tau), \tag{B9}$$

where $g(\tau)$ is a moment (couple) due to peeling at the trailing edge of the contact surface during rolling. That is,

$$g(\tau) = \lambda\zeta_A\left(m/r^3Kv_n^{1/2}\right)^{2/5}a_c\dot{\theta}. \tag{B10}$$

Although this provision for rolling dissipation is included in the equations, an investigation of its influence is not undertaken in this work, so $\lambda = 0$. For noncentral collisions, it is possible that sliding can stop and reverse; this is not true here and if sliding ends rolling must continue throughout the remainder of the contact duration.

Integration of the Equations of Motion

Equations B6, B7, and B9 are three second-order, ordinary differential equations and are integrated numerically. The method used in this paper is a Runge-Kutta-Gill technique presented by Todd (1962). The integration is straightforward, but two features deserve mention. First, if sliding ends,

1. the integration process is interrupted,
2. linear interpolation estimates the stop time,
3. the integration is repeated to the stop time,
4. the tangential force equation is changed, and
5. integration then continues from stop time.

Second, the algorithm for stopping integration at separation recognizes if the rebound velocity is too small to overcome the adhesion force, and integration continues for a short time with the sphere oscillating vertically while remaining attached to the surface.

REFERENCES

Biggs, W. D., 1965. *The Mechanical Behaviour of Engineering Materials*, Pergamon, London.

Brach, R. M., 1993. *Int. J. Impact Engr.*, 13:21–23.

Brach, R. M., 1991. *Mechanical Impact Dynamics, Rigid Body Collisions*. Wiley, New York.

Brach, R. M., 1991a. In *Computational Aspects of Impact and Penetration*, Ed. by R. F. Kulak and L. Schwer, Elmepress, Lausanne, Switzerland.

Brach, R. M. and Dunn, P. F., 1992. *J. Aerosol Sci. Technol.*, 16:51–64.

Caylor, M. J., 1993. Thesis, University of Notre Dame, Notre Dame.

Chen, Y. L., Helm, C. A., and Israelachvili, J. N. 1991. *J. Phys. Chem.* 95:10736–10747.

Dunn, P. F., Brach, R. M., and Caylor, M. J. 1995. *Aerosol Sci. Technol.*, 23:80–95.

Fichman, M., and Pnueli, D. 1985. *J. Appl. Mech.* 52:105–108.

Horn, R. G., Israelachvili, J. N., and Pribac, F. 1987. *Adhesion of Solids in Contact, J. Colloid Interface Sci.* 115:480–492.

Hunt, K. H. and F. R. E. Crossley, 1975. *J. Appl. Mech.* 440–445.

Israelachvili, J. N., 1985. *Intermolecular and Surface Forces*, Academic, New York.

Jaeger, J., 1994. *Appl. Mech. Rev.* 47:2.

Jaeger, J., 1992. Thesis, Technical University of Delft, Delft, The Netherlands.

Johnson, K. L., Kendall, K., and Roberts, A. D. 1971. *Proc. R. Soc. Lond. A*, 324:301–313.

Johnson, K. L., and Pollock, H. M. 1993. submitted.

Meyers, M. A., Murr, L. E., and Staudhammner, K. P. 1992 *Shock-Wave and High-Strain-Rate Phenomena in Materials*, Marcel Dekker, New York.

Stronge, W. J., 1990. *Proc. R. Soc. Lond.* 431:169–181.

Timoshenko, S., and Goodier, J. N. 1951. *Theory of Elasticity*, McGraw-Hill, New York.

Todd, J., 1962. *Survey of Numerical Analysis*, McGraw-Hill, New York, p. 320.

Xu, M. and Willeke, K. 1993. *Aerosol Sci. Technol.*, 18:143–155.

Received August 1, 1994; accepted January 20, 1995.